The process of rectifying electromagnetic field energy in micropower rectennas based on Schottky diodes has been investigated in this study. One of the challenges in designing such rectennas is the lack of a consistent system of quantitative criteria for selecting a rectifier diode capable of providing high conversion efficiency at ultra-low input power levels while accounting for its intrinsic and parasitic parameters. The practical relevance of this task is predetermined by the need to autonomously power Internet of Things sensors in weak electromagnetic fields.

Decomposition of loss mechanisms was performed, which made it possible to distinguish the fundamental limitations caused by the current-voltage characteristic from the frequency-dependent and parasitic diode parameters. The study was carried out using the harmonic balance method in AWR Design Environment.

The calculations showed that, in the microwatt regime, higher conversion efficiency is achieved for diodes with increased saturation current due to the dominant role of the junction threshold properties. For low-barrier structures, an increase in temperature above 50°C is accompanied by a sharp rise in reverse leakage currents, which leads to a decrease in efficiency. As the frequency increases, the junction barrier capacitance and the package parasitics increasingly limit the achievable efficiency, especially at 2.45 and 5.8 GHz.

Comparative modeling of commercial Schottky diodes revealed that, under the micropower regime, preference should be given to low-barrier structures with minimized parasitic reactances, whereas at higher input power levels the advantage may shift to structures with a medium barrier height.

Underlying the practical value of this study is the compilation of recommendations for the justified selection of components when designing battery-free power supply systems for Internet of Things sensors operating in weak electromagnetic fields

Keywords: rectenna, RF energy harvesting, Schottky diode, impedance matching, conversion efficiency

UDC 662.396.67: 621.314.6
DOI: 10.15587/1729-4061.2026.355841

SUBSTANTIATING THE CRITERIA FOR SELECTING RECTIFIER DIODES FOR LOW-POWER RECTENNA ENERGY HARVESTING SYSTEMS

Vasyl Alieksieiev
Corresponding author
PhD Student*
E-mail: vasyl.alieksieiev@nure.ua
ORCID: https://orcid.org/0000-0002-3282-5985
Dmytro Hretskykh
Doctor of Technical Sciences*
ORCID: https://orcid.org/0000-0002-2645-7872
Dmytro Havva
PhD*
ORCID: https://orcid.org/0000-0002-4033-7746
Mikhail Nesterenko
Doctor of Physical and Mathematical Sciences
Department of Physics of Ultra High Frequencies
V. N. Karazin Kharkiv National University
Svobody sq., 4, Kharkiv, Ukraine, 61022
ORCID: https://orcid.org/0000-0002-1297-9119
Olena Ivanova
PhD*
ORCID: https://orcid.org/0000-0001-9970-7951
*Department of Computer Radio Engineering and Technical Information Security Systems
Kharkiv National University of Radio Electronics
Nauky ave., 14, Kharkiv, Ukraine, 61166

Received 13.01.2026
Received in revised form 17.03.2026
Accepted 26.03.2026
Published 29.04.2026

How to Cite: *Alieksieiev, V., Hretskykh, D., Havva, D., Nesterenko, M., Ivanova, O. (2026). Substantiating the criteria for selecting rectifier diodes for low-power rectenna energy harvesting systems. Eastern-European Journal of Enterprise Technologies, 2 (8 (140)), 17–28. https://doi.org/10.15587/1729-4061.2026.355841*

1. Introduction

The evolution of the Internet of Things and wireless sensor networks has led to increased requirements for reliable autonomous power sources. In this regard, scientific research aimed at battery-free power supply and increasing the energy efficiency of conversion in weak electromagnetic fields has gained practical and scientific significance. With the mass deployment of IoT devices, the use of conventional batteries has become economically and environmentally problematic due to the need for their regular replacement and disposal [1]. Practice has revealed the need for solutions that can be applied to a large number of devices without regular service. One of the practical approaches has been the use of wireless power transfer (WPT) technologies, which are considered an important factor in enabling the energy autonomy of modern communication networks [2].

The technical implementation of the WPT concept on the consumer side is based on the use of rectennas. A rectenna is a combination of a receiving antenna and a rectifier circuit that converts the energy of an electromagnetic (EM) wave into DC power. Historically, rectennas were designed as receivers for microwave WPT systems [3] but the reduction in power consumption of microelectronics since the early 2000s has made

Copyright © 2026, Authors. This is an open access article under the Creative Commons CC BY license

the approach of harvesting energy from the ambient EM environment to power low-power sensors practically significant [4]. The Wi-Fi, GSM, DTV, and 5G infrastructure forms a dense EM coverage that can potentially serve as an ambient RF environment. At the same time, the available power flux density level is often very low (0.0017…0.86 μW/cm^2), which for typical rectenna antennas corresponds to input powers $P_{in} \approx -20\ldots-30$ dBm (10…1 μW) [5]. In this range, the conversion efficiency is significantly limited by the operating mode of the rectifier element [4]. Unlike WPT systems with a powerful microwave beam [3], at P_{in} microwatt levels, the voltage on the diode becomes comparable to its threshold properties, so the efficiency becomes strongly dependent on the input power level. At high incident power levels, efficiency values of more than 70–80% are possible [4, 6], while when approaching microwatt levels, a sharp drop in efficiency is observed [6]. This has formed a separate scientific and technical task to ensure acceptable efficiency precisely in the region of ultralow input power levels.

Therefore, designing rectennas capable of operating effectively at ultralow energy levels is a condition for increasing the sensitivity of energy harvesting systems at input powers below –20 dBm. Solving this task requires systematization of engineering criteria for selecting a semiconductor components depending on the operating mode and optimization of circuit solutions and impedance matching methods, which together make it possible to construct highly efficient systems for harvesting energy from the ambient RF environment.

Thus, research on improving the efficiency of rectennas in the microwatt range is relevant for modern wireless sensor systems. Substantiation of the criteria for selecting the components has a direct practical application.

2. Literature review and problem statement

Wireless energy transfer is considered as a set of energy transfer technologies using EM fields [2, 7]. In [7, 8], WPT methods are divided into two groups: non-radiative (inductive, resonant, capacitive coupling in the near field) and radiative (energy transfer in the Fresnel zone or far zone). For radiative systems, it is advisable to distinguish between directional energy transfer and ambient RF energy harvesting. These modes differ significantly in input power levels and requirements for the rectifier.

In work [3], the results of studies on directional energy transfer by a microwave beam in the Fresnel zone are reported. It is shown that this mode is characterized by relatively high power levels. Therefore, when choosing rectifier diodes, the breakdown and permissible current limitations are primarily taken into account. However, the selection criteria devised for this mode cannot be directly transferred to micropower energy harvesting conditions and require additional clarification. Under such conditions, the threshold properties of rectification become decisive. These conditions are typical for powering low-power devices in weak fields. In [4, 6], the results of studies on the ambient RF energy harvesting are summarized. It is noted that this mode is implemented mainly in the far zone. It is also accompanied by ultra-low power levels at the rectenna input. At such levels, even small additional losses significantly affect the useful energy in the load. Practical scenarios for the use of energy harvesting to power a large number of sensor network nodes and IoT devices are summarized in [1, 2]. In these works, the approach is considered as a technically feasible direction.

To quantify the micropower mode, the sensitivity and efficiency of rectification are used [3, 9]. The sensitivity of the rectifier is defined as the minimum input power $P_{in\,\min}$ at which a given level of DC output power P_{DC} is provided. In the small signal region $P_{in\,\min}$ is determined by the threshold nature of rectification. Therefore, the sensitivity is associated with the junction parameters and parasitic reactances of the diode package [4, 9]. The rectification efficiency is defined as the ratio of P_{DC} to the power at the input of the rectifier path P_{in}. For comparison of different works, it is important to determine the P_{in} reference point. It is set at the antenna terminals, after the matching circuit or as the available power of the source. As a result, direct comparison of the energy indicators given in different works is often complicated. In the following, P_{in} is identified with the available power P_{Avail}.

To explain the physical nature of losses during the conversion of micropower EM fields into DC power, paper [9] reports the results of studies on the mechanisms of reducing the overall efficiency along the receiving-rectifying path of the rectenna. It is shown that the total losses are formed from several components. These include losses due to the interception of EM energy by the antenna, losses due to reflection and attenuation in the matching circuits, as well as losses in the rectifier element. Additionally, effects associated with parasitic diode parameters, non-ideality of connections, and the appearance of harmonics are taken into account. The results have an important generalizing value, but in themselves they do not reduce to formalized criteria for selecting the components.

A separate class of approaches is aimed at compensating for the low level of available power at the rectenna input. To do this, the power flux density is increased or the field is localized at the receiving aperture. In [10], the use of a dynamic metasurface aperture for controlling the field distribution was analyzed. In [11], a metamaterial absorber was considered, which increases the efficiency of absorbing ambient RF signals. Such electrodynamic solutions improve the excitation conditions of the receiving part. At the same time, the requirements for the rectifier element retain a significant impact under the micropower mode. Therefore, such approaches improve the conditions for receiving energy but do not eliminate the need for a reasonable choice of the rectifier diode.

Another direction is the use of multiband and broadband rectennas [12, 13]. Such solutions make it possible to use several frequency ranges of ambient radiation and increase the total available power at the rectifier input due to the simultaneous reception of energy in several ranges. Differential solutions are used to reduce losses in the balancing nodes [14, 15]. This makes it possible to abandon the balun in the path and reduce additional losses between the antenna and the rectifier. At the same time, the above approaches mainly reduce losses in the receiving part and matching. Under the micropower mode, the limitations of the rectifier and diode retain a decisive influence on the achievable energy indicators. The indicated solutions solve important partial problems of increasing the efficiency of rectennas but do not form universal rules for choosing a diode for given conditions of the micropower mode.

At the same time, the problem of selecting a rectifier diode by its parameters has already attracted the attention of researchers, but mainly in a different context or within narrower problem statements. In particular, in [16], the influence of the intrinsic diode parameters on the efficiency of multi-band rectenna rectifiers in the range of 1.7–3.7 GHz was analyzed, and a significant influence of the intrinsic diode parameters

on the RF-to-DC conversion efficiency was shown. However, this approach is focused on statistical ranking of parameters for specific rectifier topologies and does not cover the simultaneous consideration of the temperature factor, package parasitics and regime change of the diode selection criteria in the case of transition from the micropower region to increased input power levels. In [17], the temperature dependence of rectifiers based on Schottky diodes for low-power applications was studied in detail and a significant influence of temperature on the achievable energy indicators was shown. At the same time, the temperature analysis in the study was performed for a specific series rectifier circuit and specific diodes, without generalizing the results to a system of engineering criteria for diode selection for micropower rectifiers.

Thus, the literature has already highlighted individual component problems, but the establishment of quantitative relationships between the intrinsic and parasitic parameters of Schottky diodes and the achievable efficiency and sensitivity indicators, while taking into account the frequency, input power level and operating temperature, remains unresolved. This is what determines the formulation of our study.

3. The aim and objectives of the study

The purpose of our study is to devise quantitative engineering criteria for a reasonable choice of semiconductor Schottky diodes for rectennas operating under the ambient RF energy-harvesting mode. This mode is characterized by micropower input signal levels (typically, $P_{in} \approx -20$ dBm), and the compilation of these criteria is based on establishing physically achievable limits of rectification efficiency. This will make it possible to reasonably choose the components and matching parameters for battery-free power supply of sensors in weak EM fields, taking into account the frequency and temperature of operation.

To achieve the goal, the following tasks were set:

– to perform parametric modeling of the influence of static junction parameters and temperature on the rectification efficiency in the small signal region;

– to investigate the influence of dynamic diode parameters on the rectification efficiency and determine the conditions under which they become limiting for the energy characteristics of the rectenna;

– to assess the influence of package parasitics on the energy characteristics of rectennas in the *S* and *C* bands;

– to verify the analysis results on models of commercially-available Schottky diodes of different classes and to assess the temperature stability under the ambient RF energy-harvesting mode.

4. The study materials and methods

4. 1. The object and hypothesis of the study

The object of our study is the process of converting the energy of the ultra-low-level EM field into DC power by semiconductor Schottky diodes. The principal hypothesis assumes that in the micropower range the rectification efficiency is limited by the threshold and parasitic junction parameters, which cannot be fully compensated by matching circuits. The study adopted assumptions and simplifications based on the use of idealized lossless matching circuits for an isolated assessment of the losses of the diode itself.

4. 2. Rectenna model for estimating losses in a rectifier diode

A rectenna with a single-diode half-wave rectifier was considered (Fig. 1).

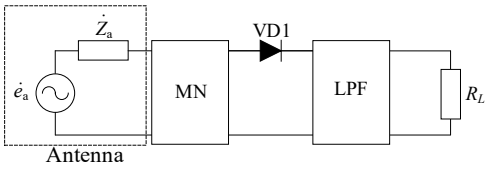

Fig. 1. Rectenna circuit with a half-wave rectifier

The matching network (MN) formed the required impedance at frequency f_0 and load conditions for harmonics, the diode VD1 performed rectification, and the low-pass filter (LPF) isolated the DC component and interfaced the load R_L. To estimate the upper limit of efficiency due to the diode, it was assumed that MN and LPF are ideal (lossless), and their impedance characteristics meet the conditions:

– the output impedance of MN at frequencies of higher harmonics ($n\omega_0$, where $n = 2, 3 ...$) is zero:

$$Z_{out}^{(1)}(n\omega_0) = \begin{cases} \infty & \text{at} \quad n = 0, \\ R_{out}^{(1)} & \text{at} \quad n = 1, \\ 0 & \text{at} \quad n > 1; \end{cases} \tag{1}$$

– the input impedance of LPF loaded on R_L must be equal to:

$$Z_{in}^{(2)}(n\omega_0) = \begin{cases} R_L & \text{at} \quad n = 0, \\ \infty & \text{at} \quad n = 1, \\ 0 & \text{at} \quad n > 1. \end{cases} \tag{2}$$

Conditions (1), (2) set an idealized regime for the fundamental component and harmonics. The energy of higher harmonics did not dissipate in passive circuits but returned to the nonlinear element. Under these assumptions, the difference between the supplied RF power and the usable P_{DC} was determined only by internal losses and conversion processes in the diode.

4. 3. Schottky diode parameters

In rectennas, diodes with a Schottky barrier are mainly used. In the microwatt range, the efficiency is largely determined by the junction parameters, package nonidealities, and temperature changes in the characteristics. Therefore, to assess their impact on the efficiency of rectennas, it is advisable to divide the diode parameters into three groups:

1. Static junction parameters. Within the resistive model, the diode behavior is described by the Shockley equation [18]

$$i = I_s\left(e^{\frac{q}{kTm}u} - 1\right). \tag{3}$$

Here, i is the current through the diode; u is the voltage at the diode junction; I_s is the saturation current; q is the electron charge; k is the Boltzmann constant; T is the absolute temperature; m is the ideality factor.

2. Dynamic and parasitic (frequency-dependent) parameters. For microwave analysis, the diode is described by an equivalent circuit (Fig. 2), which takes into account the series resistance R_s, the barrier capacitance C_j (in the micropower region, $C_j \approx C_{j0}$ is approximated), as well as the package parasitics, L_s and C_p.

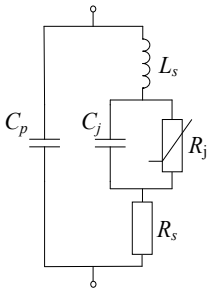

Fig. 2. Equivalent circuit of a diode

Under the matching mode, the ratio of the total radio-frequency power supplied to the diode to that part of it that is usefully absorbed directly in the nonlinear junction determines the parasitic conversion loss coefficient L_{par} [19]

$$L_{par} = 1 + \frac{R_s}{R_j} + R_s R_j \left(\omega C_{j0}\right)^2, \quad (4)$$

where $R_j = dU / dI$ – differential junction resistance.

From (4) it follows that at large values of differential resistance of the junction R_j capacitive losses increase sharply. At microwatt levels $R_j \gg 1/\omega C_{j0}$, therefore the RF current flows mainly through the barrier capacitance C_{j0}, bypassing the nonlinear junction, and the rectification efficiency decreases. Hence the requirement for the rectenna components is to choose diodes with the highest possible cutoff frequency [19]

$$f_c = \frac{1}{2\pi R_s C_{j0}}. \quad (5)$$

Reducing C_{j0} improves high-frequency performance, but usually requires a compromise with other structure parameters, in particular with R_s.

3. Temperature and operational parameters. To take into account the temperature effect in circuit modeling, the standard dependence $I_s(T)$ [20] is used

$$I_s(T) = I_s(T_{nom}) \cdot \left(\frac{T}{T_{nom}}\right)^{\frac{XTI}{m}} \cdot \exp\left[\frac{E_g}{mk}\left(\frac{1}{T_{nom}} - \frac{1}{T}\right)\right], \quad (6)$$

where T_{nom} is the nominal temperature; T is the operating temperature of the junction; E_g is the band gap; k is the Boltzmann constant; m is the ideality factor; XTI is the temperature coefficient of the saturation current.

Therefore, under conditions (1), (2), the total efficiency of the idealized rectenna was determined primarily by the junction parameters, temperature, and frequency-dependent parameters, which formed the basis for further parametric modeling and diode selection.

4. 4. Algorithm for calculating energy characteristics

The rectenna simulation was performed in the Cadence AWR Design Environment (AWRDE) within the framework of a generalized nonlinear model of the electrodynamic level of the WPT system [21–25], which reconciles the electrodynamic and circuit description. The optimization was carried out using the Source/Load Pull method, which takes into account the dependence of the rectifier input impedance on P_{in} and makes it possible to determine the maximum efficiency and justify the choice of optimal matching conditions and components. The synthesis of the optimal complex impedance within the framework of this methodology was carried out by numerical optimization of the objective function (efficiency maximization). A circuit model of a rectenna with a half-wave rectifier was built in AWRDE [26] (Fig. 3).

PORT1 in the model implemented a Thévenin equivalent source, which replaced the rectenna antenna. The excitation level was set by the available power P_{Avail} (parameter P_{wr} in PORT1) for a source with an internal resistance R_a = 50 Ohm. P_{Avail} was understood as the maximum power under conditions of ideal complex-conjugate matching. It was determined by the no-load electromotive force e_a and the active component of the antenna impedance R_a

$$P_{in} = P_{Avail} = \frac{e_a^2}{8R_a\left(f_0\right)}. \quad (7)$$

Fixing R_a = 50 Ohm was essential for correct comparison of the rectifier boundary characteristics. Changing R_a at a constant field strength would change P_{Avail}, making it impossible to estimate the efficiency of the rectifier element in isolation. Therefore, in the model, R_a was set to be constant, the excitation was determined through P_{Avail}, and during optimization, the reactive component of the source impedance X_S and the load resistance R_L were varied.

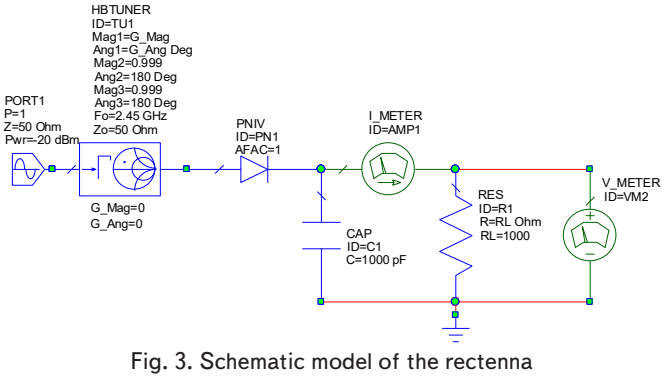

Fig. 3. Schematic model of the rectenna

The HBTUNER element (Fig. 3) simulated an ideal lossless matching network that formed the required Z_S at f_0 without changing R_a and without redistributing P_{Avail}. The optimal mode was determined by maximizing P_{DC} at a fixed P_{Avail}. For energy harvesting systems, the efficiency was determined as $\eta_r = P_{DC}/P_{Avail}$, since the approach to determining the efficiency through the absorbed power does not take into account reflection losses. The calculation was performed using the harmonic balance method with 7 harmonics. In this case, HBTUNER set lossless reactive loads for $2f_0$ and $3f_0$ (condition $|\Gamma| \approx 1$) according to (1). This was due to the fact that the main contribution of nonlinear distortions falls precisely on these harmonics [19]. Taking into account higher-order harmonics significantly complicates the implementation of real matching circuits and increases losses [27].

Capacitor C_1 (Fig. 3) performed the function of the low-pass filter. C_1 = 1000 pF was chosen from the condition of small reactance at f_0 relative to the minimum R_L

$$X_c = \frac{1}{2\pi f_0 C_1} \ll R_{L\min}. \quad (8)$$

The range of rectenna excitation levels is selected according to typical WPT scenarios [3, 12, 13]: ambient RF

energy harvesting and directional WPT. In the calculations, $P_{in} = -20...10$ dBm was assumed.

4. 5. Conditions for parametric modeling and verification

The physically achievable efficiency limit, due only to the nonlinearity of the semiconductor junction, was estimated using an idealized resistive diode model based on the Shockley equation (3) with the exclusion of frequency-dependent and parasitic parameters ($L_s = 0$, $C_p = 0$, $C_{j0} = 0$, $R_s = 0$). This formulation allowed us to separate the fundamental limitations of the current-voltage characteristic from the influence of package parasitics and the diode cutoff frequency. The determining static parameters of the model were the saturation current I_s and the ideality factor m. The variation of I_s corresponded to the change in the height of the Schottky barrier according to the Richardson-Deshman equation [18].

The maximum η_r for each P_{in} was found numerically using the Source/Load Pull method. The search for optimal source and load impedances was carried out using the Simplex optimization algorithm (Nelder-Mead method [28]). To ensure stable convergence of the optimization, the search area is limited to the values $V_{br} = 15$ V and $I_{br} = 1$ mA. These values are introduced as numerical limits, and not as datasheet parameters of a particular diode.

To analyze the threshold properties of the junction, the expression for the video resistance at zero bias was additionally used [29]

$$R_V = \frac{mkT}{qI_s} \approx \frac{0.026}{qI_s}. \quad (9)$$

At a frequency of 2.45 GHz, three typical saturation current levels were considered: $I_s = 10^{-6}$, 10^{-9}, and 10^{-14} A. The ideality factor was varied within the range $m = \{1; 1.2; 1.5\}$, where $m = 1$ corresponded to the idealized case, $m = 1.2$ – typical for commercially-available diodes, and $m = 1.5$ – a pessimistic scenario taking into account technological variation [18]. The temperature effect was evaluated for three temperature points of the industrial range: –40°C, 25°C, and 85°C.

The study of the effect of dynamic junction parameters was performed for the series resistance R_s and the barrier capacitance C_{j0}. The R_s ranges were selected based on data on commercially-available Schottky diodes: for low-barrier structures with $I_s \approx 10^{-6}$ A, $R_s = 20...50$ Ohm is typical, for medium-barrier ones with $I_s \approx 10^{-9}$ A – $R_s = 5...20$ Ohm [4]. Additionally, the reference case $R_s = 0$ Ohm was considered as the upper limit in the absence of ohmic losses. All dependences of this group were obtained at $t = 25$°C and $m = 1$. For the analysis of capacitive limitations, the values $C_{j0} = \{0.05; 0.15; 0.3; 0.5\}$ pF were considered, covering the range from low-parasitic structures to mass-market components.

The impact of the diode design on the efficiency was assessed by numerical simulation under two modes: $P_{in} = 0$ dBm (directional WPT) and $P_{in} = -20$ dBm (ambient RF energy harvesting). Three designs were considered according to reference data [30]: flip-chip package ($L_s = 0.05$ nH, $C_p = 0.05$ pF), SC-79 case ($L_s = 0.7$ nH, $C_p = 0.07$ pF) and SOT-23 case ($L_s = 2.0$ nH, $C_p = 0.15$ pF). Frequency dependences of efficiency were studied for two values of the junction capacitance of the die: $C_{j0} = 0.05$ pF and $C_{j0} = 0.15$ pF. Additionally, the dependence of the optimal load R_{Lopt} on frequency was analyzed.

Verification of the conclusions of parametric analysis at the level of SPICE models was performed for diodes of different classes of barrier structures and designs: SMS7630, MA4E20541, SMS7621, and SMS1546. The intrinsic diode parameters of the SPICE models (at $t = 25$°C) and the package parasitics are given in Table 1.

Table 1

Intrinsic diode parameters of the SPICE models and package parasitics of commercially available Schottky diodes

Diode type	Case	I_s, A	m	V_{br}, V	C_{j0}, pF	R_s, Ohm	C_p, pF	L_s, nH
SMS7630	SC-79	$5 \cdot 10^{-6}$	1.05	2	0.14	20	0.07	0.7
MA4E20541	SC-79	$3 \cdot 10^{-8}$	1.05	5	0.13	11	0.1	0.6
SMS7621	SC-79	$4 \cdot 10^{-8}$	1.05	3	0.1	12	0.07	0.7
SMS1546	SOT-23	$3 \cdot 10^{-7}$	1.04	3	0.38	4	0.15	1.5

The temperature stability of commercially-available structures was evaluated for the diode that provided the best threshold efficiency at $P_{in} = -20$ dBm. The matching network parameters were adjusted to maximum efficiency at 25°C, after which they were fixed, leaving only temperature as a variable.

5. Results of investigating the intrinsic and design limitations of rectifier diodes under the ambient RF energy-harvesting mode

5. 1. Influence of static junction parameters and temperature on the efficiency of rectenna

The results of the efficiency modeling at a frequency of 2.45 GHz are shown in Fig. 4 for three typical I_s levels (10^{-6}, 10^{-9}, 10^{-14} A). In the micropower region ($P_{in} \approx -20$ dBm), a significant difference in efficiency was found depending on I_s. For $I_s = 10^{-6}$ A, the efficiency was already about 70% at $P_{in} = -20$ dBm, while for $I_s = 10^{-14}$ A it decreased to a level of about 10–15%. In the large-signal region ($P_{in} \gtrsim 0$ dBm), the efficiency curves converged and reached approximately 90–96%.

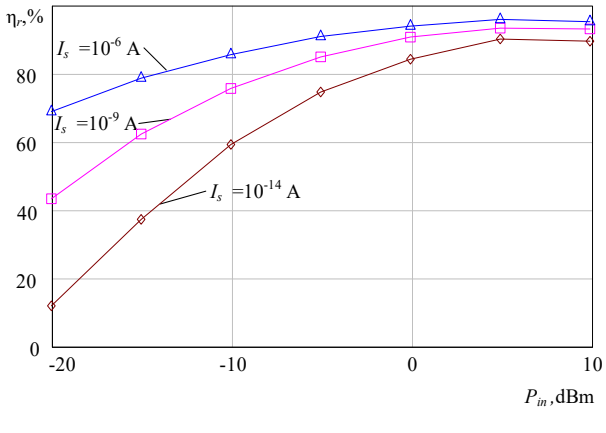

Fig. 4. Dependence of the rectification efficiency on P_{in} for diodes with different I_s under optimal matching

The next step was to evaluate the influence of the ideality factor m on efficiency (Fig. 5). According to Fig. 5, it was found that in the micropower region ($P_{in} \approx -20$ dBm) the increase in m was accompanied by a decrease in the efficiency, and this effect was enhanced with an increase in the barrier height. For the high-barrier structure (Fig. 5, *c*) when going from $m = 1$ to $m = 1.5$ the efficiency decreased from ≈ 12.2% to ≈ 0.8%. In the large-signal region ($P_{in} \approx 10$ dBm) a decrease in efficiency was also observed for $m > 1$.

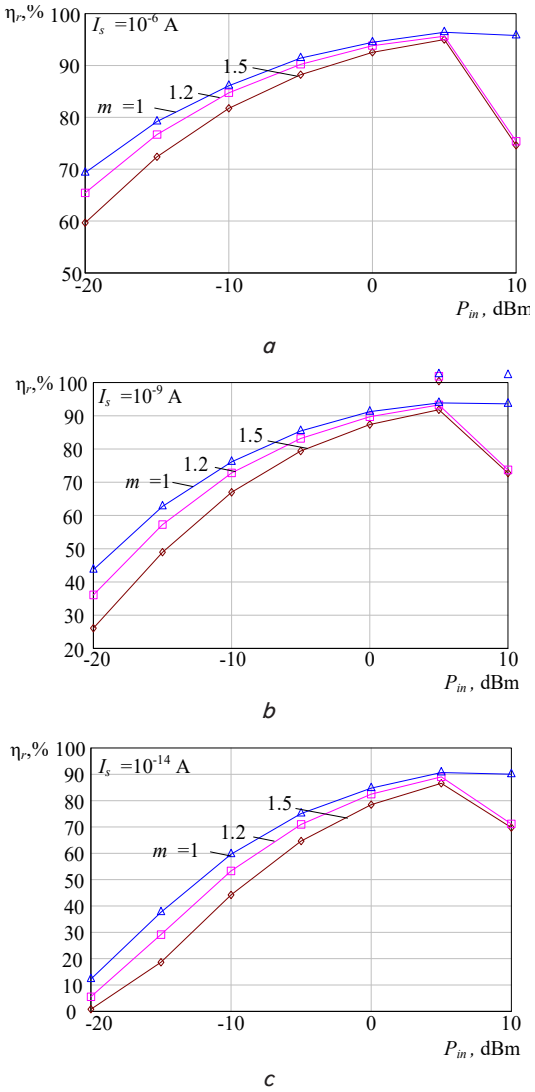

Fig. 5. Dependence of the efficiency on P_{in}: *a* – for low-; *b* – medium-; *c* – high-barrier structures for different *m*

The temperature dependences $\eta_r(P_{in})$ for three types of barrier structures are shown in Fig. 6.

The obtained dependences demonstrated the different nature of the temperature effect for diode structures of different types. For the medium-barrier structure (Fig. 6, *b*), heating to 85°C at $P_{in} = -20$ dBm increased the efficiency from ≈ 43% (at 25°C) to ≈ 64.5%. For the low-barrier structure (Fig. 6, *a*) at 85°C, the efficiency at the $P_{in} = -20$ dBm decreased to ≈ 0.12%. When the temperature was lowered to –40°C for all structures, the efficiency in the micropower region deteriorated.

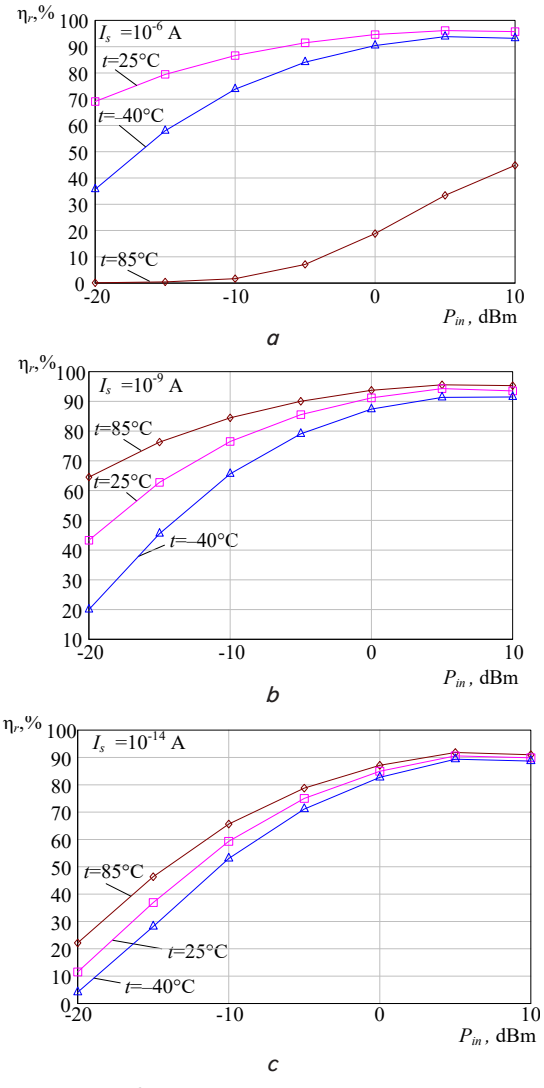

Fig. 6. Dependence of the efficiency on temperature for diodes with: *a* – low; *b* – medium; *c* – high barriers

5. 2. Influence of dynamic junction parameters on the efficiency and frequency limitations

Below, the influence of dynamic junction parameters R_s and C_{j0} on the rectification efficiency is estimated and the conditions under which they become limiting for the energy characteristics of the rectenna are determined.

According to Fig. 7, it is established that the influence of R_s is energy dependent. In the micropower region ($P_{in} \approx -20$ dBm), the change in R_s had a weak effect on the efficiency. For a low-barrier structure ($I_s = 10^{-6}$ A), the transition from $R_s = 0$ ($\eta_r \approx 69.1\%$) to $R_s = 50$ Ohm ($\eta_r \approx 68.2\%$) reduced the efficiency by approximately 1%. In the large-signal region ($P_{in} \approx 10$ dBm), the influence of R_s was amplified. For the same structure at $R_s = 50$ Ohm, the efficiency decreased by approximately 7.5% ($\eta_r \approx 95.7\% \rightarrow \eta_r \approx 88.3\%$).

Special attention is paid to the study of the influence of the barrier capacitance C_{j0} on the conversion efficiency (Fig. 8). For a low-barrier structure ($I_s = 10^{-6}$ A), with increasing C_{j0}, the efficiency at $P_{in} = -20$ dBm decreased nonlinearly. Approximately 60% at 0.05 pF and about 31% at 0.15 pF. At $C_{j0} \geq 0.3$ pF, the efficiency in the micropower region approached zero. For a medium-barrier structure ($I_s = 10^{-9}$ A), already at $C_{j0} = 0.15$ pF, the efficiency at –20 dBm dropped

to fractions of a percent, and at $C_{j0} \geq 0.3$ pF the threshold of effective operation shifted to the region of higher P_{in}.

The frequency dependence of these limitations is shown in Fig. 9.

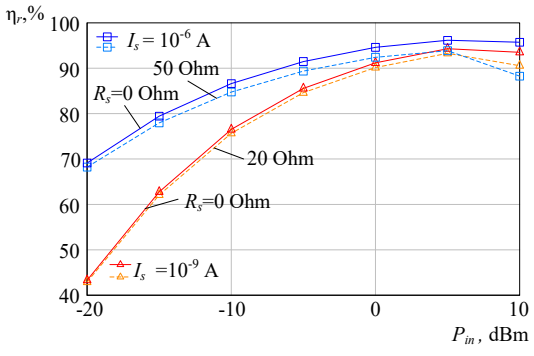

Fig. 7. Dependence of the rectification efficiency on P_{in} for diode structures with different barrier heights at different R_s

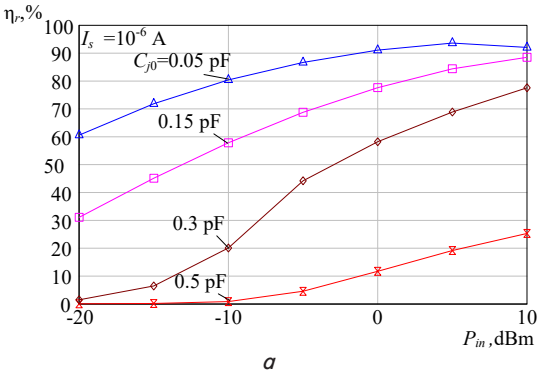

a

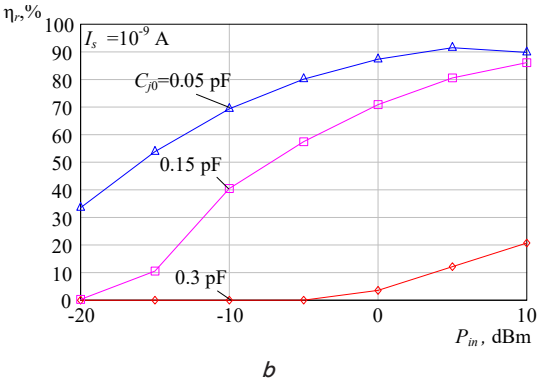

b

Fig. 8. Dependences of $\eta_r(P_{in})$ for different values of C_{j0} for: *a* – low-barrier; *b* – medium-barrier diodes at a frequency of 2.45 GHz

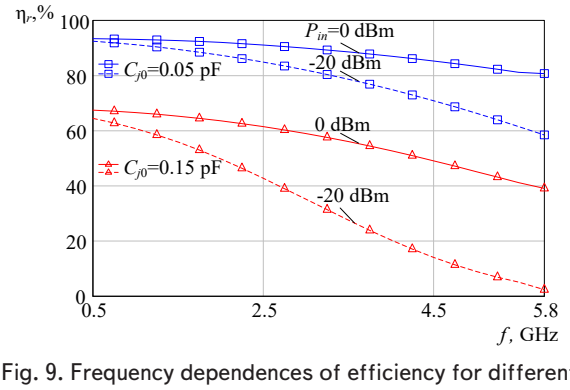

Fig. 9. Frequency dependences of efficiency for different values of junction capacitance and input power levels

Under the small-signal mode ($P_{in} = -20$ dBm) for $C_{j0} = 0.15$ pF the efficiency decreased rapidly with increasing frequency and at 5.8 GHz approached zero. At $P_{in} = 0$ dBm the decline was slower.

5. 3. Effect of package parasitics on efficiency

The frequency dependences of efficiency for $C_{j0} = 0.05$ pF and $C_{j0} = 0.15$ pF are shown in Fig. 10.

For $C_{j0} = 0.05$ pF under the $P_{in} = 0$ dBm mode, the differences between the packages were moderate. At 5.8 GHz, the transition from flip-chip to SOT-23 reduced efficiency by approximately 20%. At $P_{in} = -20$ dBm, the differences between the packages increased. At 5.8 GHz, the efficiency for SOT-23 decreased to ≈ 5.6%, while flip-chip provided ≈ 26.8%.

For $C_{j0} = 0.15$ pF, the efficiency drop in the upper part of the range was amplified. For SOT-23 at $P_{in} = -20$ dBm at 5.8 GHz, the efficiency decreased to < 3%.

The behavior of the optimal load R_{Lopt} was analyzed (Fig. 11).

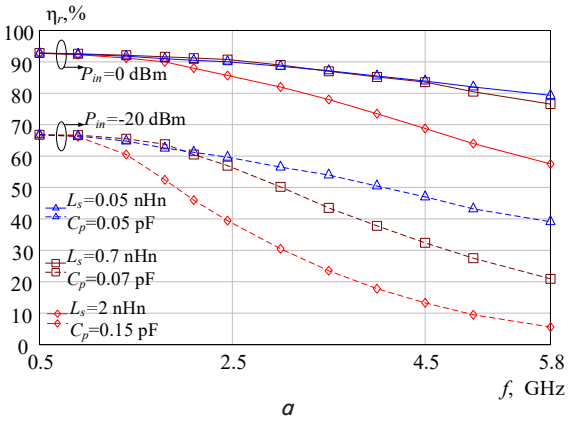

a

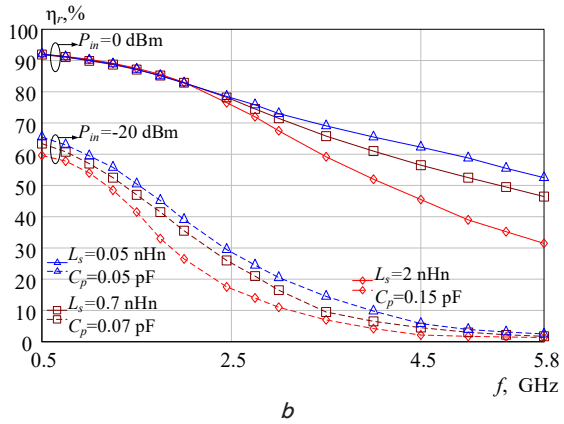

b

Fig. 10. Frequency dependences of the rectification efficiency for different diode package variants: *a* – $C_{j0} = 0.05$ pF; *b* – $C_{j0} = 0.15$ pF

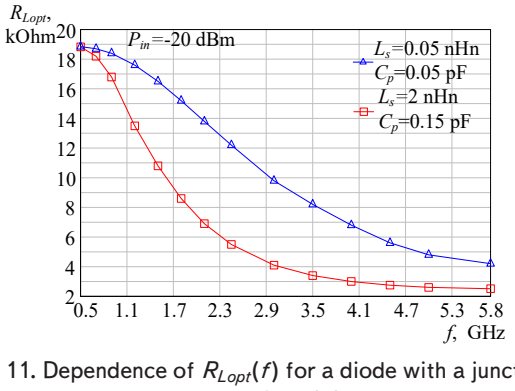

Fig. 11. Dependence of $R_{Lopt}(f)$ for a diode with a junction capacitance $C_{j0} = 0.05$ pF

According to Fig. 11, it was found that with a change in frequency, the optimal load R_{Lopt} shifted towards lower values.

5. 4. Verification of selection criteria on commercially available Schottky diodes

For commercially available diodes, the parameters of which are given in Table 1, the resulting $\eta_r(P_{in})$ dependences are shown in Fig. 12.

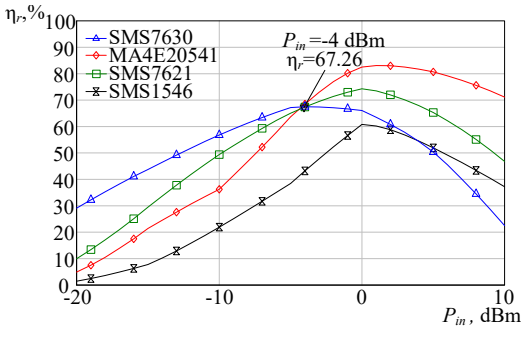

Fig. 12. Efficiency vs. P_{in} for various commercially available diodes at 2.45 GHz

According to Fig. 12, at P_{in} = –20 dBm, the SMS7630 diode provided an efficiency of about 33%, while for MA4E20541 and SMS7621 the efficiency was significantly lower (less than 8% and about 14%, respectively). The SMS1546 diode demonstrated the lowest efficiency (less than 3%). In the intermediate power range, the curves intersected at $P_{in} \approx$ –4 dBm, after which the SMS7630 efficiency began to decline. In contrast, the MA4E20541 reached a peak efficiency of more than 82% in the range of 0...2 dBm.

Since the SMS7630 diode demonstrated the best threshold efficiency at P_{in} = –20 dBm, the temperature stability was additionally evaluated (Fig. 13).

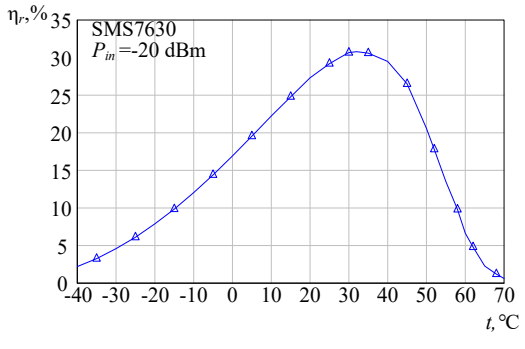

Fig. 13. Temperature dependence of the efficiency of a rectenna

The dependence had a pronounced dome-shaped character with a maximum in the range of 25...40°C. When the temperature increased above 50°C, the efficiency decreased sharply: to approximately 6% at 60°C and to a level of < 1% at 70°C.

6. Discussion of results based on parametric analysis and compilation of practical recommendations

The results allowed us to move from individual observations to a consistent system of criteria for selecting Schottky diodes for micropower rectennas. The main conclusion is that in the threshold region $P_{in} \approx$ –20 dBm, the efficiency is determined by the physical limitations of the junction and parasitic parameters. These limitations cannot be fully compensated for by external circuits in a wide range of modes.

The saturation current I_s is the basic criterion for the operability of a rectenna under the micropower mode. As shown in Fig. 4, in the range of –20...–10 dBm, an increase in I_s reduces the video resistance (9) and thereby weakens the threshold rectification properties. From an engineering point of view, this means that the first selection of the diode is advisable to do on the basis of increased I_s. At the same time, the results in Fig. 4 were obtained in an idealized resistive formulation. Therefore, they should be interpreted as an upper limit determined by the shape of the I–V characteristic.

The ideality factor m is the second most important criterion for threshold power levels. According to the results in Fig. 5, even with the same I_s, the deviation of m from 1 noticeably reduces efficiency in weak signals. At the same time, the effect is sharply enhanced for structures with small I_s. Therefore, for threshold sensitivity problems, the requirement $m \to 1$ is not only a recommendation but a necessary condition for maintaining operability in the region of –20...–10 dBm.

Temperature determines the applicability of low-barrier solutions. According to Fig. 6, low-barrier structures can lose efficiency when heated in the threshold region due to increased reverse currents. In contrast, medium-barrier structures can demonstrate better stability and even efficiency gains at the micropower point at elevated temperatures. Therefore, temperature actually acts as a criterion for choosing a barrier class. If the upper operating temperature of the object is potentially high, choosing the lowest barrier may be irrational. For room-temperature and low-temperature scenarios, low-barrier diodes provide the maximum margin in sensitivity.

The results in Fig. 7 show a fundamentally different role of the series resistance R_s under the two modes:

– in the micropower region, the contribution of R_s to the power balance is small, since losses are proportional to the square of the current, so at –20 dBm R_s is usually not a determining parameter of the rectifier performance;

– under the $P_{in} \gtrsim 0$ dBm mode, the forward currents increase to the milliampere range, and R_s becomes one of the main factors reducing the efficiency.

Therefore, the criterion of "minimizing R_s" is mandatory primarily for the directional WPT mode. For the ambient RF energy harvesting mode, the threshold performance parameters remain mainly important.

At microwave frequencies, it is C_{j0} that often determines whether the rectifier's performance is maintained under the threshold mode. According to the results in Fig. 8, 9, at the threshold point $P_{in} \approx$ –20 dBm, an increase in C_{j0} leads to the fact that the RF component of the current flows mainly through the capacitive path. As a result, the voltage at the nonlinear junction does not reach a level sufficient for effective rectification. This limitation is local at the crystal level and is not eliminated by matching. From a practical point of view, it is advisable to interpret the obtained criteria as frequency-threshold:

– up to ~1 GHz, the influence of C_{j0} is much weaker, the choice is more determined by I_s, m, and permissible R_s;

– at a frequency of 2.45 GHz at –20 dBm, diodes with small C_{j0} are required, otherwise the sensitivity deteriorates sharply;

– at a frequency of 5.8 GHz under the micropower mode, the requirements for C_{j0} become more stringent, and operability requires very small capacitance values.

Comparison of the results for commercially-available diodes with the parametric dependences shown in Fig. 4–11 shows the consistency of the formulated selection criteria. In the threshold region $P_{in} \leq -20$ dBm, the increased saturation current I_s reduces the video resistance (9) and increases the sensitivity, while at the operating frequency of 2.45 GHz, the efficiency is additionally limited by the junction capacitance C_{j0} and the package parasitics. That is why the best threshold efficiency was demonstrated by SMS7630, while the worst results were obtained for SMS1546 due to the combination of large C_{j0} and the SOT-23 package with increased package parasitics.

The simulation results shown in Fig. 10, 11 demonstrate that under the micropower mode, the design of the diode ceases to be secondary. The main mechanism for reducing efficiency is the parasitic capacitance of the package C_p, which creates a parallel capacitive path. At the same time, L_s makes a noticeable contribution through the reactance $X_L = \omega L_s$. In combination with C_p, this forms a frequency-dependent reactance of the input path, which increases the efficiency drop in the upper part of the range.

The practical conclusions from our results are as follows:

– for 2.45 GHz, compact SMD designs may be acceptable, but only under the condition of small C_{j0} and moderate C_p and L_s;

– for 5.8 GHz at –20 dBm, packages with increased C_p and L_s become a significant limitation, therefore, designs with minimal reactances or flip-chip packages are advisable;

– package parasitics shift R_{Lopt} with frequency change (Fig. 11), which should be taken into account in multi-band rectennas.

Comparative modeling of commercially available diodes (Fig. 12, 13) showed the consistency of the formed criteria at the level of real SPICE models, where all parameters act simultaneously. At the threshold point $P_{in} = -20$ dBm, diodes with increased I_s, small C_{j0}, and package parasitics (SMS7630) demonstrate an advantage. At the same time, in the zone of increased powers, the advantage passes to diodes with higher breakdown voltage and lower active losses (MA4E20541). Temperature calculation showed that for low-barrier diodes, the operating temperature range can significantly narrow due to temperature drift of the parameters.

Unlike works [31, 32] in which most attention is paid to the search for optimal matching impedances and synthesis of topologies for specific frequency ranges, our results make it possible to clearly distinguish losses caused by the fundamental nonlinearity of the junction and losses in the reactive elements of the rectifier diode package. This approach complements the temperature analysis [17] and indicates the existence of a physical efficiency limit that cannot be overcome only by circuit engineering methods without a justified change in the type of semiconductor structure. This becomes possible due to the proposed decomposition of loss mechanisms, which turns the design process of micropower systems into a predictive engineering procedure.

The proposed system of criteria makes it possible to establish a direct relationship between the parameters of the equivalent circuit of the diode (I_s, m, C_{j0}, R_s) and the energy indicators of the rectifier under the threshold mode. This is achieved by determining the limit values of reactive and nonlinear parameters, at which the efficient conversion of the energy of micropower signals into DC power is ensured. Unlike approaches based on iterative selection of components, our procedure makes it possible to screen out structures at the stage of specification analysis, whose package parasitics or junction capacitance make it impossible to obtain the target efficiency level. This approach eliminates methodological uncertainty when choosing components, enabling the predictability of the results when designing systems for ambient RF energy harvesting.

Our results make it possible to form a step-by-step procedure for selecting a diode for a micropower rectenna:

1. Formalize the application requirements. Operating frequency, minimum input power level $P_{in\,\min}$, which corresponds to the "cold start" mode. Permissible temperature range $T_{\min}...T_{\max}$, as well as the upper level $P_{in\,\max}$.

2. Selection by threshold sensitivity criteria ($P_{in} \approx -20$ dBm). First of all, structures with increased I_s and $m \to 1$ should be selected, since it is these parameters that determine the video resistance and threshold rectification properties in the small signal region.

3. Check frequency suitability by junction capacitance. For operating frequencies $f_0 \gtrsim 2$ GHz, evaluate C_{j0} as a necessary suitability criterion, since with increasing frequency, the capacitive shunting of the junction becomes significant under the "cold start" mode. For 2.45 GHz, the practical limit is the level of $C_{j0} \approx 0.15$ pF, while for 5.8 GHz, much smaller C_{j0} are required.

4. Take into account parasitic parameters of the package at high frequencies. In the range of 2.45…5.8 GHz, evaluate C_p and L_s as factors that limit the effective operating frequency and change the matching conditions. Preference is given to designs with minimized parasitic reactances.

5. Check the high-power mode ($P_{in} \gtrsim 0$ dBm). If large P_{in} levels are possible in the scenario, additionally limit the choice by R_s and V_{br}. These parameters determine the efficiency and the upper limit of the operating range under a large signal mode.

6. Final verification in nonlinear modeling. Confirm the selection by nonlinear analysis and temperature test with fixed matching parameters to assess practical efficiency.

The limitation of this study is that our analysis was carried out exclusively for half-wave rectifier circuits. Although such conditions make it possible to determine the limiting energy capabilities of individual semiconductor structures, they do not take into account the specifics of full-wave rectifier topologies and voltage doubling circuits. In such solutions, the total losses increase proportionally to the number of diodes, and the interaction of their parasitic parameters significantly changes the broadband matching conditions. This indicates the need to conduct a comparative analysis of different rectifier topologies in further studies using the developed system of criteria. A separate limitation is the use of unmodulated harmonic signals, which was appropriate for finding fundamental limits, but does not cover the effects that arise when working with real telecommunication signals of complex spectral composition.

Prospects for further research are to expand the formed criteria to multi-stage and multi-phase rectenna topologies used to increase the output power in the load. Of particular scientific interest is the verification of our results for signals with a high peak factor, which is typical for modern wireless communication standards, such as Wi-Fi or 5G. Taking into account the significant non-uniformity of the amplitude of such signals will make it possible to assess their impact on the dynamic resistance of the diode and clarify the requirements for the selection of the components for energy harvesting systems in a real ambient RF environment.

7. Conclusions

1. The influence of static junction parameters and temperature on the efficiency of small-signal rectification has been

established. In the micropower region ($P_{in} \approx -20...-10$ dBm), the efficiency is determined primarily by the threshold properties of the junction. An increase in I_s reduces the video resistance and provides higher efficiency. The requirement $m \to 1$ is a necessary condition for maintaining operability. The temperature effect is non-monotonic. In contrast to the widespread practice of unconditional selection of low-barrier diodes for rectification of weak signals, it is shown that the temperature range of operation acts as an independent criterion for choosing the barrier height. Our results are explained by the exponential dependence of current on voltage and the competition between facilitating turn-off and increasing leakage currents upon heating.

2. The influence of the dynamic parameters of the diode on the rectification efficiency was investigated and the conditions under which they become limiting for the energy characteristics of the rectenna were determined. The role of the series resistance R_s has a pronounced regime character. In the micropower region at $P_{in} \approx -20$ dBm its influence on the efficiency is insignificant, while at $P_{in} \gtrsim 0$ dBm it becomes one of the determining factors of the efficiency. The junction capacitance C_{j0} is the main microwave limitation under the "cold start" mode. At a frequency of 2.45 GHz, an increase in C_{j0} from 0.05 pF to 0.15 pF reduces the efficiency at –20 dBm from 60% to 31%. The results allowed us to determine the conditions under which the capacitive properties of the junction become limiting for effective rectification under the micropower mode. The drop in efficiency is explained by the shunting of the high-frequency current through the junction capacitance, which is not eliminated by ideal matching.

3. The influence of package parasitics on the power characteristics of rectennas in the *S* and *C* bands has been evaluated. Package parasitics set an additional frequency limit under the micropower mode. At a frequency of 5.8 GHz at –20 dBm, the efficiency decreases from 26.8% (flip-chip) to 5.6% (SOT-23). In contrast to low-frequency applications, a significant influence of the design in the micropower microwave mode was established. The decrease in efficiency is explained by the fact that the parasitic capacitance C_p acts as an additional shunt path, and in combination with L_s shifts the optimal load, making standard packages ineffective.

4. Our results were verified on commercially available Schottky diode models; their temperature stability was assessed. A comparison at 2.45 GHz confirmed the formulated selection criteria. The SMS7630 diode provides the highest efficiency at the threshold point of –20 dBm (33%) but is limited by low V_{br}. In contrast, the MA4E20541 provides a higher efficiency of over 82% in the range of 0...2 dBm. The decrease in the efficiency of low-barrier diodes at temperatures above 50°C is explained by the dominance of reverse leakage currents. Unlike empirical methods of component selection, the verification demonstrated the consistency of the devised engineering criteria, which turns the process of a priori selection of the components for battery-free sensor power supply into an algorithmic procedure.

Conflicts of interest

The authors declare that they have no conflicts of interest in relation to the current study, including financial, personal, authorship, or any other, that could affect the study and the results reported in this paper.

Funding

The study was conducted without financial support.

Data availability

All data are available in the main text of the manuscript.

Use of artificial intelligence

The authors declare the use of generative artificial intelligence (Gemini 1.5 Pro model) during the preparation of this manuscript. In accordance with the GAIDeT taxonomy, tasks were delegated to the tool under full human supervision. In particular, AI was used during the preparation of the section "Literature review and problem statement" for basic systematization of the text, as well as for checking the uniform style of presentation, editing grammar, and eliminating lexical repetitions throughout the manuscript. Additionally, the tool was used during the writing of the abstract to ensure a given range of characters with spaces. All literary sources were selected and processed by the authors completely independently. Scientific conclusions, modeling results, and research methodology are exclusively the author's intellectual property and were formed without the participation of AI. The edited text underwent a final authors' proofreading to guarantee the accuracy of radio engineering terminology and preservation of physical content. In addition, in order to control the results obtained in the studies on all tasks, the authors conducted a comparative analysis of the calculated results with test and individual numerical or experimental data known from the literature. The authors bear full responsibility for the final manuscript and scientific results. Generative AI tools do not meet the criteria for authorship, are not indicated as co-authors and are not responsible for the final results.

Authors' contributions

Vasyl Alieksieiev: Conceptualization. Methodology. Software. Investigation. Formal analysis. Visualization. Writing – original draft; **Dmytro Hretskykh**: Conceptualization. Methodology. Supervision. Project administration. Writing – review & editing; **Dmytro Havva**: Validation. Formal analysis. Writing – review & editing; **Mikhail Nesterenko**: Nesterenko: Data curation. Formal analysis; **Olena Ivanova**: Validation. Writing – review & editing.

References

1. Tran, L.-G., Cha, H.-K., Park, W.-T. (2017). RF power harvesting: a review on designing methodologies and applications. Micro and Nano Systems Letters, 5 (1). https://doi.org/10.1186/s40486-017-0051-0
2. Nikoletseas, S., Yang, Y., Georgiadis, A. (Eds.) (2016). Wireless Power Transfer Algorithms, Technologies and Applications in Ad Hoc Communication Networks. Springer International Publishing. https://doi.org/10.1007/978-3-319-46810-5

3. Shinohara, N. (2013). Wireless Power Transfer via Radiowaves. John Wiley & Sons. https://doi.org/10.1002/9781118863008
4. Hemour, S., Wu, K. (2014). Radio-Frequency Rectifier for Electromagnetic Energy Harvesting: Development Path and Future Outlook. Proceedings of the IEEE, 102 (11), 1667–1691. https://doi.org/10.1109/jproc.2014.2358691
5. Costanzo, A., Masotti, D. (2017). Energizing 5G: Near- and Far-Field Wireless Energy and Data Trantransfer as an Enabling Technology for the 5G IoT. IEEE Microwave Magazine, 18 (3), 125–136. https://doi.org/10.1109/mmm.2017.2664001
6. Valenta, C. R., Durgin, G. D. (2014). Harvesting Wireless Power: Survey of Energy-Harvester Conversion Efficiency in Far-Field, Wireless Power Transfer Systems. IEEE Microwave Magazine, 15 (4), 108–120. https://doi.org/10.1109/mmm.2014.2309499
7. Zhang, Z., Pang, H., Georgiadis, A., Cecati, C. (2019). Wireless Power Transfer – An Overview. IEEE Transactions on Industrial Electronics, 66 (2), 1044–1058. https://doi.org/10.1109/tie.2018.2835378
8. Popovic, Z. (2017). Near- and far-field wireless power transfer. 2017 13th International Conference on Advanced Technologies, Systems and Services in Telecommunications (TELSIKS), 3–6. https://doi.org/10.1109/telsks.2017.8246215
9. Gu, X., Hemour, S., Wu, K. (2022). Far-Field Wireless Power Harvesting: Nonlinear Modeling, Rectenna Design, and Emerging Applications. Proceedings of the IEEE, 110 (1), 56–73. https://doi.org/10.1109/jproc.2021.3127930
10. Smith, D. R., Gowda, V. R., Yurduseven, O., Larouche, S., Lipworth, G., Urzhumov, Y., Reynolds, M. S. (2017). An analysis of beamed wireless power transfer in the Fresnel zone using a dynamic, metasurface aperture. Journal of Applied Physics, 121 (1). https://doi.org/10.1063/1.4973345
11. Fowler, C., Silva, S., Thapa, G., Zhou, J. (2022). High efficiency ambient RF energy harvesting by a metamaterial perfect absorber. Optical Materials Express, 12 (3), 1242. https://doi.org/10.1364/ome.449494
12. Visser, H. J., Vullers, R. J. M. (2013). RF Energy Harvesting and Transport for Wireless Sensor Network Applications: Principles and Requirements. Proceedings of the IEEE, 101 (6), 1410–1423. https://doi.org/10.1109/jproc.2013.2250891
13. Pinuela, M., Mitcheson, P. D., Lucyszyn, S. (2013). Ambient RF Energy Harvesting in Urban and Semi-Urban Environments. IEEE Transactions on Microwave Theory and Techniques, 61 (7), 2715–2726. https://doi.org/10.1109/tmtt.2013.2262687
14. Saito, K., Nishiyama, E., Toyoda, I. (2022). A 2.45- and 5.8-GHz Dual-Band Stacked Differential Rectenna With High Conversion Efficiency in Low Power Density Environment. IEEE Open Journal of Antennas and Propagation, 3, 627–636. https://doi.org/10.1109/ojap.2022.3171035
15. Chandravanshi, S., Sarma, S. S., Akhtar, M. J. (2018). Design of Triple Band Differential Rectenna for RF Energy Harvesting. IEEE Transactions on Antennas and Propagation, 66 (6), 2716–2726. https://doi.org/10.1109/tap.2018.2819699
16. Contreras, A., Urdaneta, M. (2021). Analysis of Variance of the Diode Parameters in Multiband Rectifiers for RF Energy Harvesting. Radioengineering, 30 (1), 150–156. https://doi.org/10.13164/re.2021.0150
17. Paz, H. P. D., Silva, V. S. D., Diniz, R., Trevisoli, R., Capovilla, C. E., Casella, I. R. S. (2023). Temperature Analysis of Schottky Diodes Rectifiers for Low-Power RF Energy Harvesting Applications. IEEE Access, 11, 54122–54132. https://doi.org/10.1109/access.2023.3281794
18. Sze, S. M., Ng, K. K. (2006). Physics of Semiconductor Devices. John Wiley & Sons. https://doi.org/10.1002/0470068329
19. Maas, S. A. (2003). Nonlinear Microwave and RF Circuits. Boston: Artech House, 608. Available at: https://us.artechhouse.com/Nonlinear-Microwave-and-RF-Circuits-Second-Edition-P1097.aspx
20. Quarles, T., Newton, A. R., Pederson, D. O., Sangiovanni-Vincentelli, A. (1993). SPICE3 Version 3f3 User's Manual. Berkeley, 145. Available at: http://www.gianlucafiori.org/appunti/Spice_3f3_Users_Manual.pdf
21. Gretskih, D. V., Luchaninov, A. I., Vishniakova, J. V., Katrich, V. A., Nesterenko, M. V. (2018). Electrodynamic Model of a Wireless Power Transmission System. 2018 XXIIIrd International Seminar/Workshop on Direct and Inverse Problems of Electromagnetic and Acoustic Wave Theory (DIPED), 80–85. https://doi.org/10.1109/diped.2018.8543290
22. Luchaninov, A. I., Gretskih, D. V., Gomozov, A. V., Katrich, V. A., Nesterenko, M. V. (2019). Electrodynamic Approach to Designing WPT Systems with Accounting for Non-system Interactions. 2019 IEEE 2nd Ukraine Conference on Electrical and Computer Engineering (UKRCON), 107–111. https://doi.org/10.1109/ukrcon.2019.8879788
23. Gretskih, D., Luchaninov, A., Katrich, V., Nesterenko, M. (2019). Electrodynamic Approach to Designing Wireless Power Transfer Systems (Internal System Processes). 2019 International Conference on Information and Telecommunication Technologies and Radio Electronics (UkrMiCo), 1–6. https://doi.org/10.1109/ukrmico47782.2019.9165536
24. Gretskih, D., Luchaninov, A., Katrich, V., Nesterenko, M., Gomozov, A. (2019). Extemal Parameters of Wireless Power Transmission Systems. 2019 XXIVth International Seminar/Workshop on Direct and Inverse Problems of Electromagnetic and Acoustic Wave Theory (DIPED), 117–121. https://doi.org/10.1109/diped.2019.8882592
25. Alieksieiev, V., Gretskih, D., Luchaninov, A., Lykhograi, V., Shcherbina, A. (2021). Applying the Electrodynamic Approach to Modeling Wireless Power Transmission Systems. 2021 IEEE 26th International Seminar/Workshop on Direct and Inverse Problems of Electromagnetic and Acoustic Wave Theory (DIPED), 111–115. https://doi.org/10.1109/diped53165.2021.9552254
26. AWR Design Environment Platform (2026). Cadence Design Systems. Available at: https://www.cadence.com/en_US/home.html
27. Roberg, M., Falkenstein, E., Popovic, Z. (2012). High-efficiency harmonically-terminated rectifier for wireless powering applications. 2012 IEEE/MTT-S International Microwave Symposium Digest, 1–3. https://doi.org/10.1109/mwsym.2012.6259641
28. Nelder, J. A., Mead, R. (1965). A Simplex Method for Function Minimization. The Computer Journal, 7 (4), 308–313. https://doi.org/10.1093/comjnl/7.4.308

29. The Zero Bias Schottky Detector Diode: Application Note 969. San Avago Technologies, 6. Available at: https://people.ee.ethz.ch/~mzahner/PPS-EMrad/material/literature/RF-Detectors_Receivers/The%20Zero%20Bias%20Schottky%20Detector%20Diode%20(Avago%20AN%20969).pdf
30. SMS7630 Series. Surface Mount Mixer and Detector Schottky Diodes. Available at: https://www.skyworksinc.com/Products/Diodes/SMS7630-Series
31. El Mattar, S., Baghdad, A., Ballouk, A. (2022). A 2.45/5.8 GHz high-efficiency dual-band rectifier for low radio frequency input power. International Journal of Electrical and Computer Engineering (IJECE), 12 (3), 2169. https://doi.org/10.11591/ijece.v12i3.pp2169-2176
32. Bhatt, K., Kumar, S., Kumar, P., Tripathi, C. C. (2019). Highly Efficient 2.4 and 5.8 GHz Dual-Band Rectenna for Energy Harvesting Applications. IEEE Antennas and Wireless Propagation Letters, 18 (12), 2637–2641. https://doi.org/10.1109/lawp.2019.2946911